Diabetes, Metabolic Syndrome and Obesity: Targets and Therapy Dovepress
open access to scientific and medical research

Open Access Full Text Article

ORIGINAL RESEARCH

Estrogen receptor inhibition enhances cold-induced adipocyte beiging and glucose tolerance

This article was published in the following Dove Press journal:
Diabetes, Metabolic Syndrome and Obesity: Targets and Therapy

Kfir Lapid[1,2]
Ajin Lim[1]
Eric D Berglund[3,4]
Yue Lu[2]

[1]Department of Developmental Biology, [2]Division of Endocrinology, Department of Internal Medicine, [3]Advanced Imaging Research Center, [4]Department of Pharmacology, University of Texas Southwestern Medical Center, Dallas, TX, USA

Background: Low estrogen states, exemplified by postmenopausal women, are associated with increased adiposity and metabolic dysfunction. We recently reported a paradox, in which a conditional estrogen receptor-alpha (ERα) mutant mouse shows a hyper-metabolic phenotype with enhanced brown/beige cell formation ("browning/beiging").

Hypothesis: These observations led us to consider that although systemic deficiency of estrogen or ERα in mice results in obesity and glucose intolerance at room temperature, cold exposure might induce enhanced browning/beiging and improve glucose metabolism.

Methods and results: Remarkably, studying cold-exposure in mouse models of inhibited estrogen signaling - ERαKO mice, ovariectomy, and treatment with the ERα antagonist Fulvestrant - supported this notion. ERα/estrogen-deficient mice demonstrated enhanced cold-induced beiging, reduced adiposity and improved glucose tolerance. Fulvestrant was also effective in diet-induced obesity settings. Mechanistically, ERα inhibition sensitized cell-autonomous beige cell differentiation and stimulation, including β3-adrenoreceptor-dependent adipocyte beiging.

Conclusion: Taken together, our findings highlight a therapeutic potential for obese/diabetic postmenopausal patients; cold exposure is therefore predicted to metabolically benefit those patients.

Keywords: adipose tissue, post-menopause, brown fat, obesity, diabetes

Introduction

Obesity and diabetes afflict many in Western civilizations, and are also a feature of estrogen deficiency.[1,2] Hence, postmenopausal women are prone to show signs of increased adiposity and metabolic dysfunction.[1,2] Accordingly, obesity and metabolic dysfunction develop in pre-clinical estrogen-deficient models, including ERαKO and ovariectomized (OVX) female mice.[3,4] Hormone replacement therapy (eg, estradiol administration) is successful in reversing metabolic dysfunction in rodent models and postmenopausal women.[1,5] Yet, hormone replacement therapy increases the risk of cardiovascular diseases and breast cancer.[6,7] Nonetheless, we recently uncovered an unanticipated function of ERα in systemic metabolism.[8] We found that mutant mice, with low estrogen signaling in the adipose lineage, display a lean phenotype, an improved glucose tolerance and increased metabolic rates.[8] This paradoxical phenotype appeared secondary to an augmented brown/beige adipocyte differentiation, which appears to occur at the expense of white adipocyte differentiation.[8] Whereas the primary function of white adipocytes is to store excess energy intake, brown/beige adipocytes convert extra calories into thermal energy, thereby ameliorating diabetes and obesity.[9–13] Cold-exposure and sympathetic adrenergic signals are well-established stimuli that activate brown adipose tissue (BAT) and trigger formation of beige

Correspondence: Kfir Lapid
Division of Endocrinology, Department of Internal Medicine, University of Texas Southwestern Medical Center, 5323 Harry Hines Boulevard, Dallas, TX 75390-9133, USA
Tel +1 214 648 6804
Fax +1 214 648 8917
Email Kfir.Lapid@utsouthwestern.edu

submit your manuscript | www.dovepress.com
DovePress
http://doi.org/10.2147/DMSO.S190752

adipocytes;[9–11] the latter form within white adipose tissue (WAT). Indeed, cold temperatures are capable of ameliorating diabetes and obesity in rodents and human patients.[9–11,14–16] Since our aforementioned findings suggest that ERα regulates beiging/browning, we tested whether a browning/beiging stimuli, for example cold-exposure, may improve metabolic outcomes in mouse models of estrogen or estrogen receptor deficiencies. That is, mice with inhibited estrogen receptor are more susceptible to cold-induced browning/beiging effects, which do not normally occur at room temperature. To test our notion, we undertook a series of studies on independent and complementary models: whole-body ERαKO female mice, OVX females, and treatment with the potent estrogen receptor antagonist Fulvestrant ("Faslodex"™).[17] In all models, we observed decreased adiposity and improved metabolic outcomes, which were secondary to enhanced cold-induced beiging and BAT activation. We also probed the effects in a primary beige cell culture and demonstrated a cell-autonomous beiging following estrogen receptor inhibition. Finally, estrogen receptor inhibition appeared to enhance beiging also via β3-adrenoreceptor upregulation and activation.

Materials and methods

Mice

WT strains include ICR(CD1) (for chronic Fulvestrant administration in mice on normal chow) and C57BL/6 mice (all other in vivo experiments). ERαKO mice were generously provided by Dr. Deborah J. Clegg.[18] Experiments were performed on 4–6-month-old female mice as indicated. The mice were housed in a temperature-controlled environment using a 12:12 light/dark cycle, and chow and water were provided ad libitum. The mice were fed either normal chow (4% fat, Harlan-Teklad, Madison, WI) or high-fat diet (58% fat with sucrose, Research Diets, New Brunswick, NJ). Food intake was measured by weighing crude chow per mouse per cage. For cold experiments, mice were placed in a 6 °C cold-chamber for 7 days or maintained at RT (23 °C). Body temperatures were measured using a rectal probe. Bilateral ovariectomy and sham operations were done in C57BL/6 females as instructed in our standard operating procedure. Fat/lean content/mass were measured using a minispec MQ10 NMR Analyzer (Bruker, Billerica, MA). Fulvestrant (40 mg/kg/injection, Sigma, St. Louis, MO) or vehicle (DMSO) were dissolved in sunflower oil; acute administration – two intraperitoneal injections beginning 3 days prior to cold-exposure, or chronic administration - four intraperitoneal injections beginning 30 days prior to cold-exposure. CL-316,243 (1 mg/kg/day, Tocris Bioscience, Minneapolis, MN) was dissolved in H_2O; three daily subcutaneous injections, mice were analyzed a day after. Mice were fasted for ~2 hr at RT prior to euthanization in most experiments, however, prior to glucose uptake assay and glucose/insulin tolerance tests, they were fasted for ~5 hr at RT. For glucose and insulin tolerance tests, 1.25 mg glucose (Sigma) or 0.3–0.75 mU Humalog (Lilly, Indianapolis, IN)/g mouse weight were injected intraperitoneally; blood glucose levels were measured from the cut tail at the indicated intervals using Contour blood glucose monitoring (Bayer, Mishawaka, IN). Glucose uptake assay: a jugular vein catheter was surgically implanted in mice one week prior to cold-exposure, using previously described procedures.[19,20] At the end of cold-exposure, mice were injected with a bolus of 13 μCi of [^{14}C]-2-deoxy-D-glucose (2-DG) in the jugular vein catheter. Blood samples were obtained at indicated intervals post-injection, after which mice were euthanized, and tissues were collected. Previously described procedures and calculations were used to determine plasma and tissue radioactivity, and to measure tissue-specific glucose uptake.[18,19] Other measurements were performed in the UTSW Mouse Metabolic Phenotyping Core: sera insulin, triglycerides and cholesterol and liver triglycerides. All animal procedures were ethically approved by the UT Southwestern Medical Center institutional animal care and use committee (IACUC) – protocols 2010–0015, 2015–100991 and 2016–101336. The UT Southwestern Medical Center IACUC follows the policies of the USDA Animal Welfare Act and the Association for Assessment and Accreditation of Laboratory Animal Care International.

Cell culture

Stromal vascular (SV) fraction was obtained from subcutaneous adipose depots of two-month old mice as described.[8,20,21] Isolated SV cells were cultured in DMEM supplemented with 10% FBS, 100 units/mL penicillin, 100 mg/mL streptomycin and 25 ng/mL Amphotericin B (Sigma). White adipogenesis was induced as described.[8,21] Beige adipogenesis was induced similarly, except for an addition of 5 nM indomethacin (Sigma) and 2 nM T3 (Sigma).[20] Fulvestrant (1 μM, Sigma), Estradiol (1 μM, Sigma), CL-316,243 (Tocris Bioscience), SR59230A (1 μM, Sigma), Propranolol (1 μM, Cayman Chemical, Ann Arbor, MI) or vehicles (ethanol, H_2O or DMSO in equivalent dilutions) were added to confluent cells with each media change. To induce thermogenic genes, cells were treated with 10 μM Forskolin (Sigma), 1 μM

Norepinephrine (dissolved in H_2O with 0.125 mM ascorbic acid, Sigma) or 1 μM CL-316,243–8 hr for RNA isolation or 24 hr for immunostaining. "Sub-optimal beige media" - IBMX and Dexamethasone (Sigma) were removed. Oil Red O staining, Nile Red staining and immunostaining were done as described.[8,21] Relative changes in cAMP levels were measured using cAMP-Glo™ Max Assay (Promega, Madison, WI) following induction in PBS and IBMX (500 μM, Sigma) with or without 10 μM Forskolin for 15 min.

Histology, immunohistochemistry and fluorescent immunostaining

Tissues were formalin-fixed, paraffin-embedded, sectioned and stained with haematoxylin and eosin (H&E) as described.[21] Immunohistochemistry and immunofluorescence were done as described.[20,21] Following de-paraffinization, the immunostaining procedure of paraffin-embedded tissue sections was similar to that of frozen tissues and cultured cells. Primary antibodies: rabbit anti-UCP1 (1:200, Abcam, Cambridge, MA), rabbit anti-ERα (1:200, Abcam), rabbit anti-mouse β3-adrenergic-receptor (1:200, Abcam), mouse anti-PCNA (1:200, Millipore, Burlington, MA) and goat-anti-Perilipin (1:200, BD Biosciences, San Jose, CA). Secondary antibodies: Goat/Donkey anti- rabbit/mouse conjugated with AlexaFluor-488/Cy3, and Donkey anti-goat conjugated with Cy5 (1:500, Jackson ImmunoResearch, West Grove, PA). DAPI (1:500, Fluka, Milwaukee, WI). Nile-red (1 μg/mL, Sigma). Bright-field and fluorescent images were collected on: Olympus inverted IX70 microscope, Olympus upright BX40 microscope, Leica inverted DMi8 microscope or Leica upright DM6 microscope. An independent researcher reviewed slides to confirm results.

Unilocularity index

Random photomicrographs were taken from regions of interest in histological H&E sections of paraffin-embedded adipose tissues. The regions of interest are represented by multilocular-rich areas in adipose tissues, such as anterior inguinal adipose depots (ie SWAT) and medial perigonadal adipose depots (ie VWAT). The photos were converted into 8-bit high-contrast grayscale images, followed by segmentation using the "Montpellier RIO Imaging Adipocytes Tools" plugin and the Watershed algorithm in ImageJ.[22] Unilocular cells were defined as cells having lipid droplets of ≥350 μm.[2,23] Unilocularity index – area covered by large lipid droplets as a fraction of total image area, excluding non-adipose tissue (eg, blood vessels, mesothelium, space between adipose tissue nodules). Reduced unilocularity index indicates that larger area is covered by small lipid droplets and adipocyte cytoplasm, inferring thereof increased multilocularity.

Quantitative Real-time PCR

Total RNA was extracted from adipose tissues or cultured cells as described.[8,20] cDNA synthesis and qPCR analysis of gene expression were done as described.[8,20] qPCR values were normalized to β-actin. Primer sequences are presented in Table S1 (provided by IDT, Skokie, IL).

Statistical analyses and data presentation

Statistical significance was assessed by two-tailed Student's *t*-test, one-way ANOVA analysis, area under curve and linear regression analyses. Error bars indicate S.E.M. All experiments were repeated at least 3 times. Variable sample size may result from the fact that different cohorts were used for different sets of experiments. Calculations were done, and figures were generated using Microsoft Excel 2016, GraphPad Prism 7, ImageJ 1.5, CorelDraw X6 and ChemDraw 15.

Results

Whole-body ERαKO mice reduce adiposity and increase glucose tolerance following cold-exposure

We previously reported that ERα plays alters adipose lineage specification: adipose lineage-restricted (stem cells to mature adipocytes) ERα mutants display increased beige adipocyte formation and BAT activity together with blunted white adipocyte formation.[8] These observations led us to consider that browning/beiging associated with ERα disruption in the adipose lineage might also be present in whole-body ERαKO mice under the right conditions. Induction of browning/beiging in ERαKO females, for example by cold-exposure,[9] is therefore predicted to result in fat loss and improved metabolism, despite their prominent obesity and metabolic dysfunction.[3,24] To test this possibility, we placed 4-month-old WT and ERαKO female mice in a cold-chamber for a week or kept them at room-temperature (RT). Cold-exposed ERαKO females significantly reduced body weight, fat content and fat mass, when compared to their counterparts at RT, whereas cold-exposed WT females did not (Figure 1A–C). Further, the size and mass of subcutaneous and visceral fat depots were significantly decreased in cold-exposed ERαKO

females (~3 fold-change) compared to cold-exposed WT females (Figures 1D, S1A–B). As expected, cold-exposed females ate more than females at RT, however, ERαWT and ERαKO females exhibited similar food intake (Figure S1C). Of note, cold-exposure did not affect lean mass and weight of other organs (Figure S1D and E). Since obesity is often associated with manifestation of diabetes, we tested whether the reduction in adiposity of ERαKO females is also associated with improvement of the metabolic profile. Although at RT, we detected hyperglycemia in ERαKO females, cold-exposure significantly lowered serum glucose levels, which were similar to the levels measured in cold-exposed WT females (Figure 1E). We also detected similar reductions in serum cholesterol and triglyceride levels in cold-exposed ERαKO females (Figure S1F). We then performed glucose and insulin tolerance tests at RT or following a week of cold-exposure. Although at RT, ERαKO females demonstrated reduced glucose and insulin tolerance versus WT counterparts, cold-exposure markedly increased their glucose and insulin tolerances (Figures 1F and S1G). Cold-exposure did not affect the glucose tolerance of WT females, and only marginally improved their insulin tolerance, however, WT females still performed better at these tests compared to the ERαKO counterparts (Figures 1F and S1G). Of note, high insulin levels remained intact following cold-exposure (Figure S1H). Altogether, we found that upon cold-exposure, female ERαKO mice exhibited a significant reduction in adiposity and serum glucose levels together with increased glucose and insulin tolerance. We had similar observations of reduction in adiposity and metabolic improvement in cold-exposed ERαKO males (not shown). These data suggest that in the absence of ERα mice are more sensitive to the metabolic-positive effects of cold, in contrast to their diabetic phenotype at RT.

Whole-body ERαKO mice exhibit enhanced cold-induced beiging

According to our hypothesis, the cold-mediated effects on adiposity and glucose metabolism are secondary to an enhanced beiging in ERαKO females. At RT, obese ERαKO females were featured with large adipocytes in the subcutaneous WAT (SWAT) (Figure 1G). At cold, histological examination of SWAT pointed to emergence of multilocular adipocytes, which were more abundant in ERαKO females compared to their WT counterparts (Figure 1G and Table S2). We did not notice any clear differences in the emergence of multilocular adipocytes in the visceral WAT (VWAT) at cold (Figure S2A and Table S2). At RT, interscapular classical BAT (or BAT) appeared "whiter" in ERαKO females, however, cold-exposure restored its appearance to a normal morphology (Figure 1H). UCP1 expression is a hallmark of brown and beige multilocular adipocytes.[9,13] UCP1 immunohistochemistry of SWAT indicated an increased abundance of $UCP1^+$ beige cells in cold-exposed ERαKO females as compared to cold-exposed WT females (Figure S2B). A key piece of molecular evidence to support the suggested increased beiging is that compared to cold-exposed WT females, cold-exposed ERαKO females presented elevated mRNA levels of brown/beige cell markers in SWAT, including UCP1 (Figure 1I). In contrast to SWAT, VWAT did not present an enhanced cold-induced beiging by gene expression (Figure S2C). Nonetheless, we additionally detected a slight elevation of gene expression in BAT of ERαKO females (Figure 1J). Even though we did not detect $UCP1^+$ cells at RT (Figure S2B), ERαKO females exhibited increased basal mRNA levels of UCP1 in SWAT (Figure S2D, applies to other genes too – not shown), but neither in BAT nor in VWAT (not shown). Although increased BAT activity is often associated with a rise in body temperature,[13] cold-exposed ERαKO females exhibited reduced body temperature in a manner similar to WT females (Figure S2E). We had similar observations of enhanced cold-induced beiging in ERαKO males (not shown). Our data therefore suggest that reduced adiposity and improved glucose metabolism in cold-exposed ERαKO mice are secondary to enhanced cold-induced browning/beiging.

Ovariectomized females reduce adiposity and increase glucose tolerance following cold-exposure

In addition to a mouse model lacking the receptor ERα, a model lacking the ligand estrogen might serve as a complementary model to test the notion of enhanced cold-induced beiging. A common pre-clinical model in rodents for postmenopause is surgical removal of the ovaries, which results in lower levels of circulating estradiol.[25] OVX female rodents gradually develop obesity and glucose intolerance, consistent with metabolic manifestations of diabetic postmenopausal women.[2,4,5,26] Female mice were sham or OVX operated at 2-month of age. Three months later, after allowing OVX females to develop a diabetic phenotype, we placed sham and OVX mice in a cold-chamber for a week or kept them at RT. As expected, at RT, body weight, fat content and mass were higher in OVX females versus sham females (Figure 2A–C). Following cold-exposure, OVX females

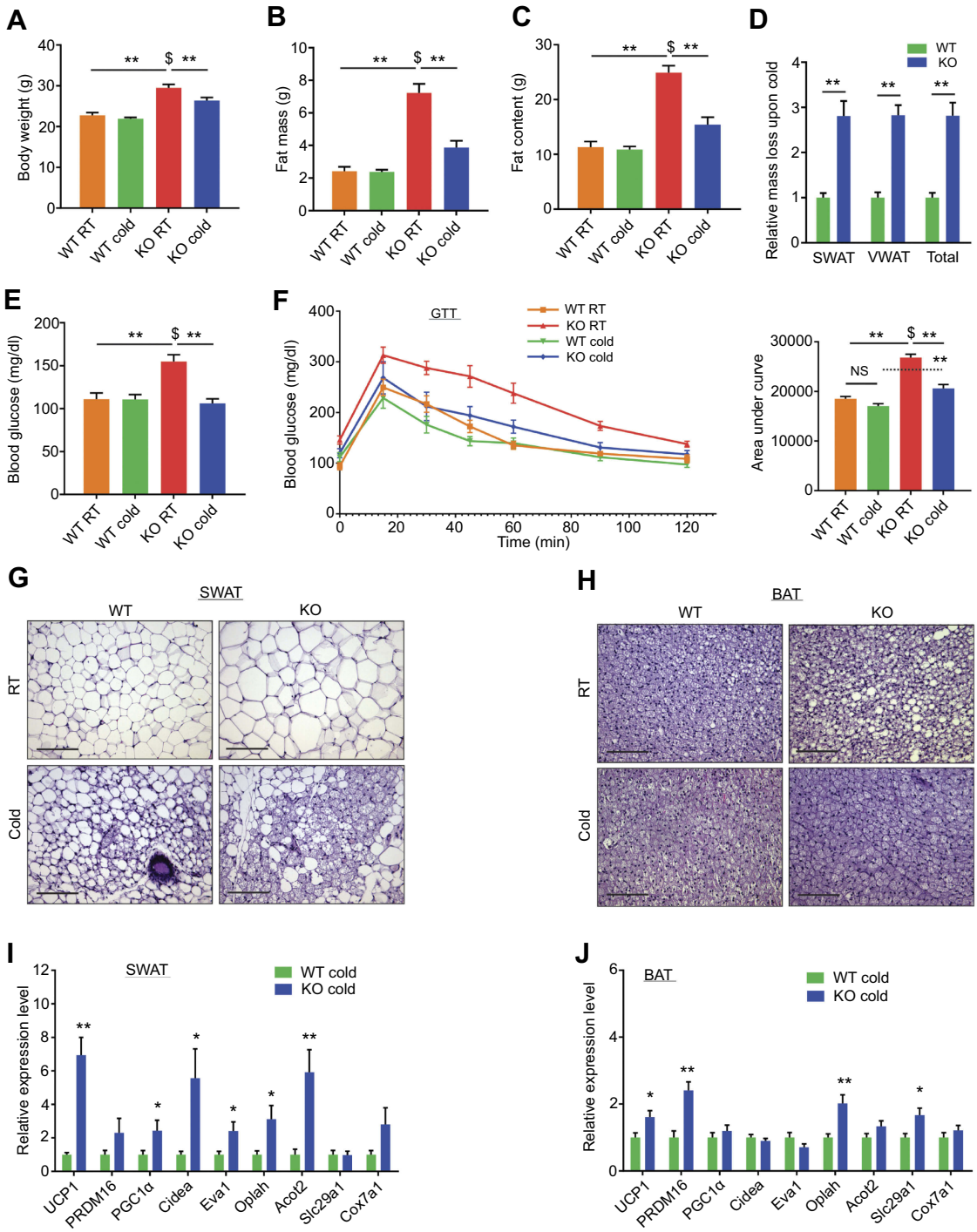

Figure 1 Whole-body ERαKO mice reduce adiposity, increase glucose tolerance and exhibit enhanced beiging following cold-exposure. Four-month-old female ERαWT (WT) and ERαKO (KO) mice were subjected to cold-exposure (6 °C) for 7 days or maintained at RT (23 °C). (**A**) Body weight, n≥12. (**B**) Fat mass by NMR, n≥8. (**C**) Fat content by NMR, n≥8. (**D**) Relative fat mass loss in SWAT and VWAT compartments of WT and KO females were calculated according to white adipose depot weights (see Figure S1B): SWAT = Cold (2*IGW + ISCW) – RT (2*IGW + ISCW); VWAT = Cold (2*PGW + 2*RPW + MWAT) – RT(2*PGW + 2*RPW + MWAT), n≥8. (**E**) Blood glucose levels of WT and KO females, n≥6. (**F**) Glucose tolerance tests were performed in WT and KO females at RT (a week prior to cold-exposure) and immediately after cold-exposure. Mice were fasted, i.p. injected with 1.25 g/kg glucose, and their glucose levels were monitored, n≥8. Inset – areas under curve. (**G**–**H**) Representative H&E-stained histological sections of SWAT (**G**) and BAT (H), n≥8. (**I**–**J**) Relative mRNA levels, quantified by qPCR, of brown/beige adipocyte markers expressed in SWAT (IGW, **I**) and BAT (**J**) of WT and KO females at cold, n≥6. Scale bars =100 μm. Error bars indicate S.E.M. Statistical significance assessed by two-tailed student's *t*-test, **p*<0.05, ***p*<0.01, NS, not significant; and one-way ANOVA test, $^{\$}p$<0.01.

significantly reduced body weight, fat content and fat mass, when compared to their counterparts at RT, while sham females only marginally (Figure 2A–C). Further, the size and mass of subcutaneous and visceral fat depots were significantly decreased in cold-exposed OVX females (~4.5 fold-change) compared to cold-exposed sham females (Figures S3A–B and 2D). As expected, cold-exposed females ate more than females at RT, however, sham and OVX females exhibited similar food intake (Figure S3C). Interestingly, the liver, which is fatty in OVX females,[27] was reduced in weight following cold-exposure (Figure S3D). Yet, cold-exposure did not affect lean mass and weight of other organs (Figure S3E and F). Next, we evaluated whether the metabolic state of the OVX females could be improved in a similar manner to ERαKO females (Figure 1). While at RT, we detected hyperglycemia in OVX females, cold-exposure significantly lowered serum glucose levels, which were similar to values in cold-exposed sham females (Figure 2E). We also detected similar reductions in serum cholesterol and triglyceride levels in cold-exposed OVX females (Figure S3G). We subsequently performed glucose and insulin tolerance tests at RT or following a week of cold-exposure. While at RT, OVX females demonstrated glucose intolerance when compared to the sham counterparts and cold-exposure markedly increased their glucose tolerance (Figure 2F). Unlike the positive effect of cold-exposure on insulin tolerance of ERαKO females (Figure S1G), cold-exposure did not affect this parameter in OVX females (Figure S3H). Cold-exposure also did not affect the insulin tolerance of sham females, and only marginally their glucose tolerance, however, sham females still performed better at these tests, compared to the OVX counterparts (Figures 2F and S3H). Of note, high insulin levels remained intact following cold-exposure (Figure S3I). Altogether, we found that upon cold-exposure, OVX females exhibited a significant reduction in adiposity and glucose levels together with increased glucose tolerance, suggesting that lower circulating estrogen sensitizes these mice to the metabolic-positive effects of cold.

Ovariectomized females exhibit enhanced cold-induced beiging

In line with findings in ERαKO females (Figure 1), we asked whether we also observe enhanced cold-induced beiging in OVX females? At RT, obese OVX females were featured with large adipocytes in the SWAT and VWAT (Figures 2G and S4A). At cold, histological examination of SWAT pointed to emergence of multilocular adipocytes, which were more abundant in OVX females compared to their sham counterparts (Figure 2G and Table S2). We did not detect such histological differences in VWAT (Figure S4A and Table S2). At RT, BAT appeared "whiter" in OVX females, however, cold-exposure restored its appearance to a normal morphology (Figure S4B). UCP1 immunohistochemistry of SWAT indicated an increased abundance of UCP1^{+} beige cells in cold-exposed OVX females as compared to cold-exposed sham females (Figure S4C). In line with enhanced cold-induced beiging in ERαKO females (Figure 1I), cold-exposed OVX females presented elevated mRNA levels of brown/beige cell markers in SWAT as compared to cold-exposed sham females (Figure 2H). We additionally detected a slight elevation of gene expression in VWAT and BAT of cold-exposed OVX females (Figures S4D and 2I). As opposed to ERαKO females, OVX females showed similar basal mRNA levels of UCP1 in SWAT at RT (Figure S2D and S4E). Despite increased browning/beiging at cold, OVX females reduced their body temperature in a similar manner to sham females (Figure S4F). Aligned with reduction in liver weight (Figure S3D), cold-exposure resulted in correction of estrogen deficiency-associated hepatosteatosis (Figures 2J and S4G). Our data therefore suggest that reduced adiposity and improved glucose metabolism in OVX mice at cold are secondary to enhanced cold-induced browning/beiging.

Fulvestrant enhances beiging in vitro and in vivo

To test whether estrogen receptor inhibition enhances beiging in a cell-autonomous manner, we utilized a primary beige adipocyte culture. We isolated and cultured SWAT-derived stromal vascular (SV) cells, which are known to contain adipose progenitors.[21] Once the cells reached confluency, we exposed them to beige adipogenic media for a week and then activated them with Forskolin.[20] Since ERα-deficient progenitors have compromised adipogenesis,[8] we treated primary cells with the potent estrogen receptor antagonist Fulvestrant.[17,28] Unlike other selective estrogen receptor modulators (SERM), Fulvestrant is capable of ERα downregulation,[29,30] which we confirmed in vitro (Figure 3A). Treatment with Fulvestrant during differentiation increased the number of UCP1^{+} beige cells in culture as compared to controls (Figure 3B). Gene expression analysis of beige cell markers supported the notion of a cell-autonomous beiging (Figure 3C). Notably, Fulvestrant did not affect adipogenesis in general (Figure S5A), and was insufficient to trigger de novo adipogenesis in non-adipogenic media (not

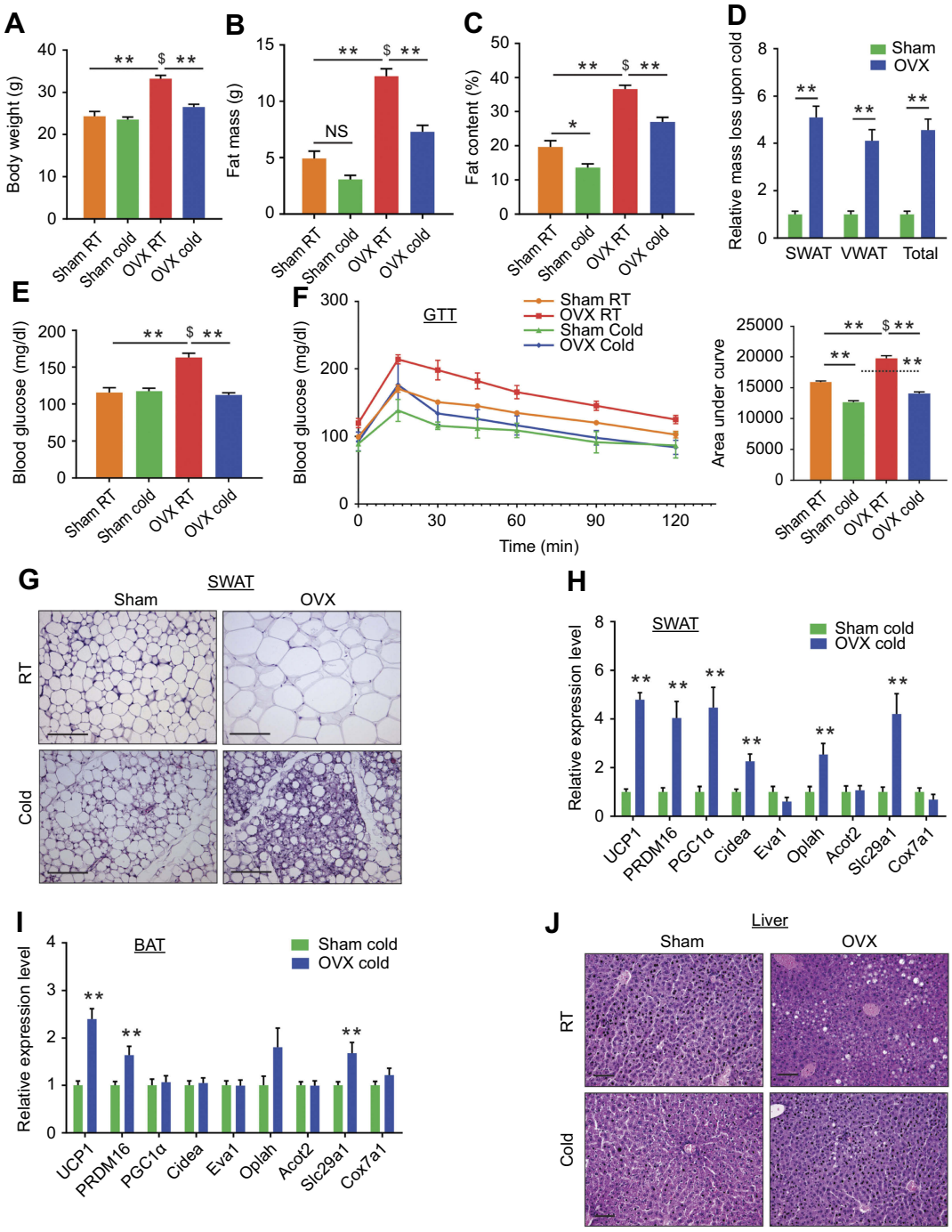

Figure 2 Ovariectomized females reduce adiposity, increase glucose tolerance and exhibit enhanced beiging following cold-exposure. Two-month-old female mice underwent sham operation or ovariectomy (OVX), 3 months later, both groups were either subjected to cold-exposure (6 °C) for 7 days or maintained at RT (23 °C). (**A**) Body weight, n≥11. (**B**) Fat mass by NMR, n≥6. (**C**) Fat content by NMR, n≥6. (**D**) Relative fat mass loss in SWAT and VWAT compartments of Sham and OVX females were calculated according to white adipose depot weights (see Figure S3B): SWAT = Cold (2*IGW + ISCW) – RT (2*IGW + ISCW); VWAT = Cold (2*PGW + 2*RPW +MWAT) – RT (2*PGW + 2*RPW + MWAT), n≥8. (**E**) Blood glucose levels of Sham and OVX females, n≥8. (**F**) Glucose tolerance tests were performed in Sham and OVX females at RT (a week prior to cold-exposure) and immediately after cold-exposure. Mice were fasted, i.p. injected with 1.25 g/kg glucose, and their glucose levels were monitored, n≥9. Inset – areas under curve. (**G**) Representative H&E-stained histological sections of SWAT, n≥8. (**H**–**I**) Relative mRNA levels, quantified by qPCR, of brown/beige adipocyte markers expressed in SWAT (IGW) (**H**) and BAT (**I**) at cold, n≥6. (**J**) Representative H&E-stained histological sections of the liver. Scale bars =100 μm. Error bars indicate S.E.M. Statistical significance assessed by two-tailed Student's *t*-test, **p*<0.05, ***p*<0.01, NS, not significant; and one-way ANOVA test, $^{\$}p$<0.01.

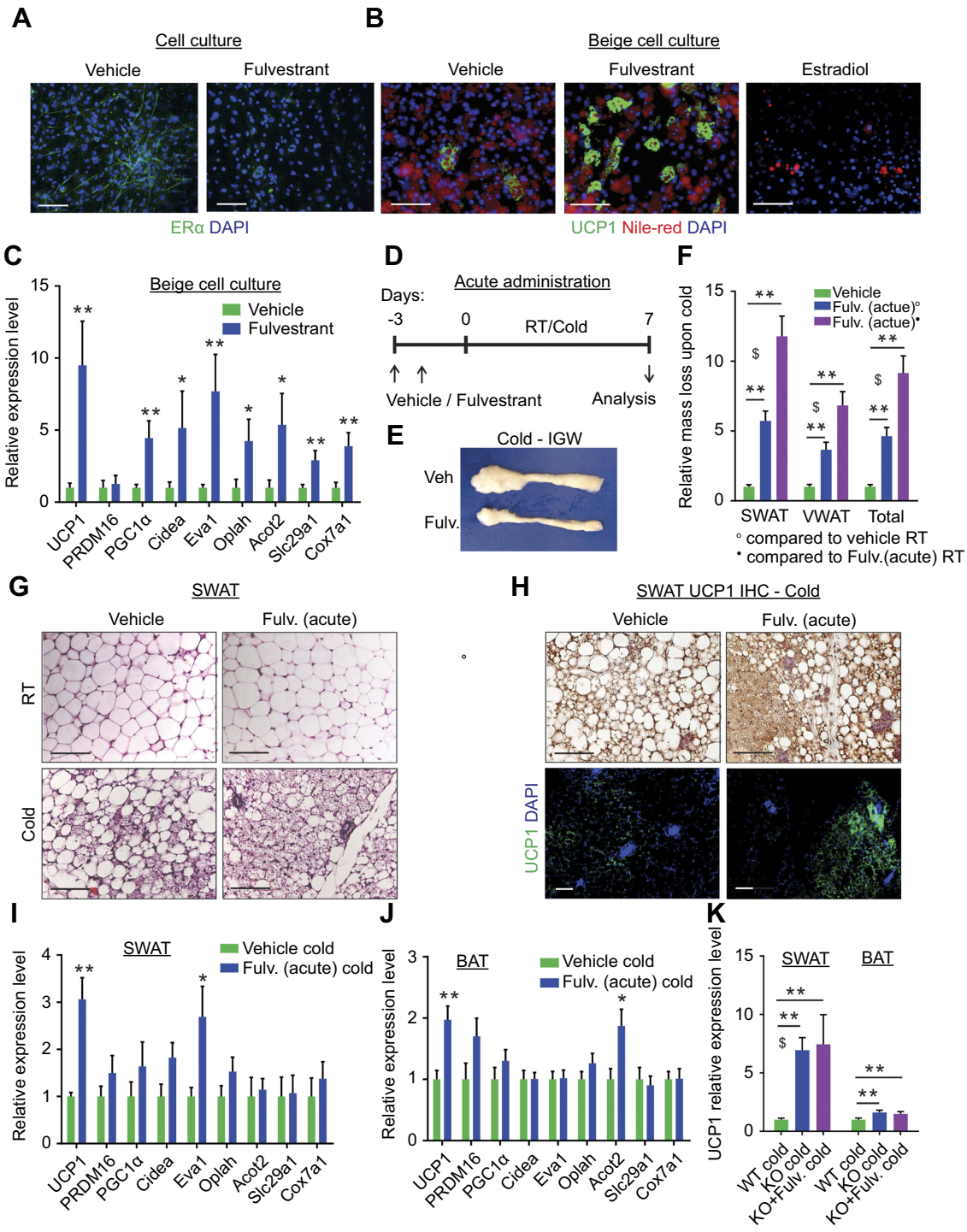

Figure 3 Fulvestrant enhances beiging in vitro and in vivo. (**A**–**C**) Stromal-vascular (SV) cells were isolated from SWAT of two-month-old females. (**A**) Confluent cells were treated daily with a vehicle or Fulvestrant for 48 hr, and immunostained for ERα expression. (**B–C**) Confluent cells were induced with beige adipogenic media in the presence of vehicles, Fulvestrant or Estradiol. A week later, beige cells were activated with Forskolin. Beiging was assessed by UCP1 immunostaining (**B**) or relative mRNA levels, quantified by qPCR, of brown/beige adipocyte markers, n≥7 (C). Nile Red stains lipid droplets. (**D–J**) Acute administration: Four-month-old WT females were given a vehicle or 40 mg/kg/injection Fulvestrant as described in (D), then they were subjected to cold-exposure (6 °C) for 7 days or maintained at RT (23 °C). (**E**) Representative photographs of IGW adipose depots of vehicle-treated and Fulvestrant-treated females at cold. (**F**) Relative fat mass loss in SWAT and VWAT compartments of vehicle-treated and Fulvestrant-treated females were calculated according to white adipose depot weights (see Figure S5F): SWAT = Cold (2*IGW + ISCW) – RT (2*IGW + ISCW); VWAT = Cold (2*PGW + 2*RPW + MWAT) – RT(2*PGW+2*RPW+MWAT), n≥7. (**G**) Representative H&E-stained histological sections of SWAT, n≥7. (**H**) UCP1 immunohistochemistry (upper lane) and immunofluorescence (lower lane) - representative sections of SWAT at cold. (**I–J**) Relative mRNA levels, quantified by qPCR, of brown/beige adipocyte markers expressed in SWAT (IGW) (I) and BAT (J) at cold, n≥5. (**K**) Vehicle or Fulvestrant administration in four-month-old ERαKO (KO) females in a similar manner to the WT females, as described in (**D**), followed by cold-exposure (6 °C) for 7 days. Relative mRNA levels, quantified by qPCR, of UCP1 in SWAT (IGW) and BAT, n≥5. Histological morphology confirms no difference in beiging between vehicle-treated and Fulvestrant-treated KO mice (not shown). Scale bars =100 μm. Error bars indicate S.E.M. Statistical significance assessed by two-tailed Student's *t*-test, **p*<0.05, ***p*<0.01; and one-way ANOVA test, $*p*<0.01.

shown). Fulvestrant was also incapable of converting white adipocytes to beige adipocytes (Figure S5B), implying it enhances adipocyte beiging rather than inducing interconversion. Conversely, the ERα ligand, estradiol, has been reported to suppress in vitro white adipogenesis;[31] In support, our results show that estradiol suppressed in vitro beiging (Figures 3B and S5C–D), but not in the presence of Fulvestrant (Figure S5D). Next, we tested whether estrogen receptor inhibition by Fulvestrant can also enhance cold-induced beiging in vivo. We acutely treated 4-month-old females with Fulvestrant or vehicle, and then placed them in a cold-chamber for a week or kept them at RT (Figure 3D). Following cold-exposure, vehicle-treated and Fulvestrant-treated females did not show reduction in body weight (Figure S5E). Nevertheless, reduction in adiposity was more significant in Fulvestrant-treated females versus vehicle-treated females (Figures 3E–F and S5F). This cold-induced reduction in adiposity was not associated with altered food intake (Figure S5G). Acute Fulvestrant treatment did not affect the weight of other organs (not shown). In accordance with cold effects on ERαKO females (Figure 1G and Table S2), acute Fulvestrant treatment augmented the emergence of multilocular adipocytes in SWAT at cold (Figure 3G and Table S2), but not in VWAT (Figure S5H and Table S2). At RT, acute Fulvestrant treatment had no effect on the histological morphology of WAT or BAT (Figures 3G and S5H, not shown). UCP1 immunohistochemistry of SWAT at cold indicated an increased abundance of $UCP1^+$ beige cells in Fulvestrant-treated females as compared to vehicle-treated females (Figure 3H). Furthermore, at cold, Fulvestrant-treated females presented slightly elevated mRNA levels of brown/beige cell markers in SWAT and BAT compared to vehicle-treated females (Figure 3I and J). We had similar observations of enhanced cold-induced beiging in Fulvestrant-treated males (not shown). As a control experiment, acute administration of Fulvestrant in ERαKO mice did not result in any additive effect on cold-induced beiging (Figure 3K, not shown). This supports the hypothesis that the effect of Fulvestrant on beiging is ERα-dependent. Taken together, ERα inhibition via Fulvestrant treatments mimics the effects of ERα absence, enhancing beiging in vitro and in vivo.

Chronic Fulvestrant treatment reduces adiposity and enhances cold-induced beiging

Acute Fulvestrant treatment moderately enhanced cold-induced beiging/browning in female mice. To test the beiging potential of chronic Fulvestrant treatments, we used an outbred mouse strain of ICR(CD1) that is known to be heavier than the inbred C57Bl/6 strain used so far in this study.[32]We treated female mice with Fulvestrant or vehicle for a month at RT (Figure 4A), considering a long pharmacokinetic half-life of the drug.[33] Fulvestrant treatment was effective in downregulating ERα in WAT and BAT (Figure S6A–C). We monitored the mice during the chronic Fulvestrant treatment - there were no notable changes in body weight, fat mass, fat content or lean mass (Figure S6D–F). Then, we placed these mice in a cold-chamber for a week or kept them at RT. Following cold-exposure, Fulvestrant-treated females significantly reduced body weight, fat content and fat mass, when compared to their counterparts at RT, while vehicle-treated females only marginally (Figures 4B–D and S6D–F). Further, the size and mass of subcutaneous and visceral fat depots were significantly decreased upon cold-exposure in Fulvestrant-treated females (~2 fold-change) compared to vehicle-treated controls (Figures 4E–G). This cold-induced reduction in adiposity was not associated with altered food intake (Figure S6H). Of note, Fulvestrant did not affect lean mass and weight of other organs (Figure S6G and I). In contrast to the blood glucose lowering effect of cold-exposure in ERαKO and OVX females (Figures 1E and 2E), we did not observe any differences in serum glucose levels (Figure 4H); possibly because these mice are not hyperglycemic at RT. Although systemic glycemia did not change, WAT depots demonstrated increased glucose uptake (2.3–3.7 fold-change) in Fulvestrant-treated females when compared to vehicle-treated females in the cold (Figure 4I). Other organs showed no difference in tissue glucose uptake, including BAT (Figure 4I). This might be due to the timing of the experiment or preference for fatty acid use by cold-activated brown adipocytes.[16] At cold, histological examination pointed at striking differences between Fulvestrant-treated females and vehicle-treated females – not only in SWAT, but VWAT also displayed a high abundance of multilocular adipocytes (Figure 5A–B and Table S2). At RT, chronic Fulvestrant treatment had no impact on the histological morphology of WAT or BAT (Figure 5A–B, not shown). UCP1 immunohistochemistry of SWAT and VWAT at cold indicated an increased abundance of $UCP1^+$ beige cells in Fulvestrant-treated females compared to vehicle-treated females (Figure 5C and D). Furthermore, at cold, Fulvestrant-treated females presented elevated mRNA levels of brown/beige cell markers in SWAT, VWAT and BAT versus vehicle-treated females (Figure 5E and G). At RT, Fulvestrant-treated females exhibited

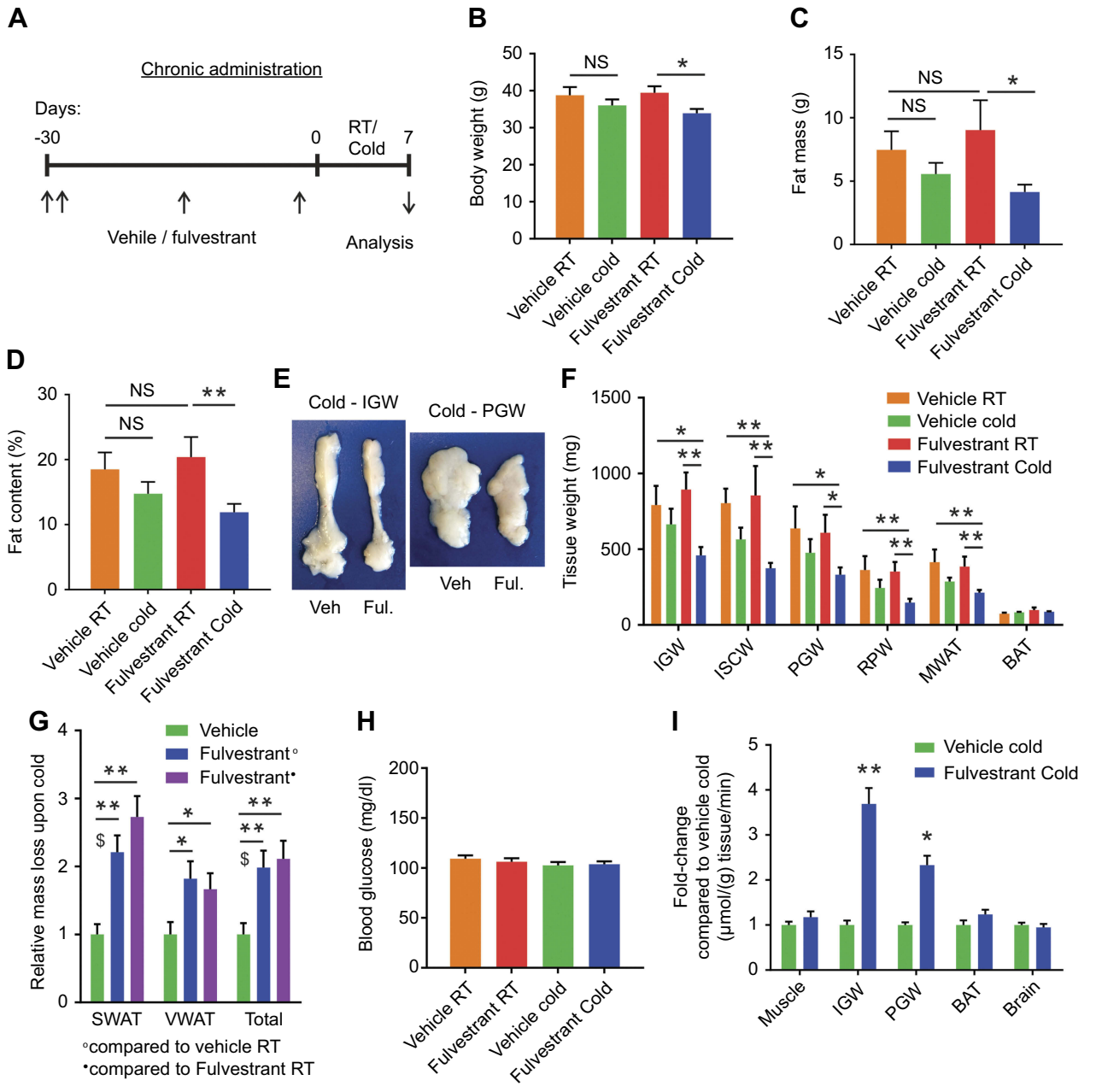

Figure 4 Chronic Fulvestrant treatment reduces adiposity. (**A–I**) Chronic administration: four-month-old WT ICR(CD1) females were given a vehicle or 40 mg/kg/injection Fulvestrant for a month, then they were subjected to cold-exposure (6 °C) for 7 days or maintained at RT (23 °C), as described in (**A**). (**B**) Body weight, n≥6. (**C**) Fat mass by NMR, n≥6. (**D**) Fat content by NMR, n≥6. (**E**) Representative photographs of IGW and PGW adipose depots of vehicle-treated and Fulvestrant-treated females at cold. (**F**) Weight of indicated fat depots in vehicle-treated and Fulvestrant-treated females: SWAT - IGW and ISCW; VWAT - PGW, RPW and MWAT; and intrascapular BAT, n≥6. (**G**) Relative fat mass loss in SWAT and VWAT compartments of vehicle-treated and Fulvestrant-treated females were calculated according to white adipose depot weights (see Figure 4F): SWAT = Cold (2*IGW + ISCW) – RT (2*IGW + ISCW); VWAT = Cold (2*PGW + 2*RPW + MWAT) – RT (2*PGW + 2*RPW + MWAT), n≥6. (**H**) Blood glucose levels of vehicle-treated and Fulvestrant-treated females, n≥6. (**I**) In vivo glucose uptake assay, based on radiolabeled 2-DG administration, in vehicle-treated and Fulvestrant-treated females upon cold-exposure (see methods for further details), n≥5. Error bars indicate S.E.M. Statistical significance assessed by two-tailed Student's *t*-test, **p*<0.05, ***p*<0.01, NS, not significant; and one-way ANOVA test, $^{\$}p$<0.01.

increased basal mRNA levels of UCP1 in SWAT (Figure S7A, applies to other genes too – not shown). Thus, chronic Fulvestrant pre-treatment enhanced cold-induced beiging to a larger extent than acute Fulvestrant pre-treatment. In addition, we observed a physiological outcome that we did not observe in ERαKO and OVX females – while vehicle-treated females reduced their body temperature upon cold-exposure, Fulvestrant-treated females retained a higher body temperature (Figure 5H). Monitoring the females at the course of cold-exposure showed that they

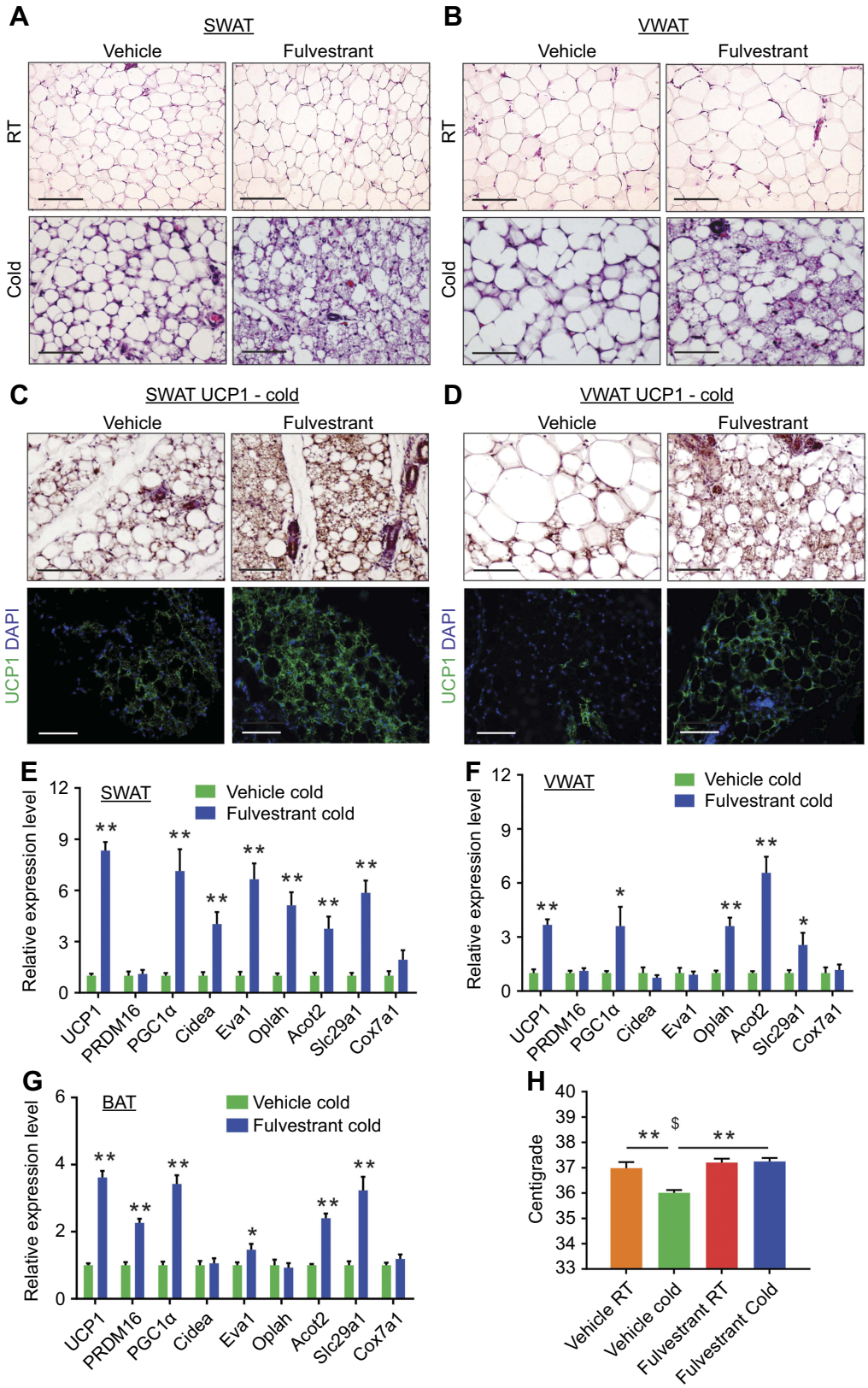

Figure 5 Chronic Fulvestrant treatment enhances cold-induced beiging. Chronic administration, as described in Figure 4A. (**A–B**) Representative H&E-stained histological sections of SWAT (**A**) and VWAT (**B**), n≥7. (**C–D**) UCP1 immunohistochemistry (upper lane) and immunofluorescence (lower lane) - representative sections of SWAT (**C**) and VWAT (**D**) at cold. **(E–G)** Relative mRNA levels, quantified by qPCR, of brown/beige adipocyte markers expressed in SWAT (IGW) (**E**), VWAT (PGW) (**F**) and BAT (**G**) at cold, n≥8. (**H**) Body temperature (rectal probe) of vehicle-treated and Fulvestrant-treated females at RT and cold, n≥6. Scale bars =100 μm. Error bars indicate S.E.M. Statistical significance assessed by two-tailed Student's *t*-test, **p*<0.05, ***p*<0.01; and one-way ANOVA test, $^{\$}p$<0.01.

were more resistant to cold exposure (Figure S7B), likely implying involvement of enhanced thermogenesis. In conclusion, chronic Fulvestrant treatment in female mice followed by cold-exposure leads to reduced adiposity, enhanced cold-induced beiging of WAT, increased glucose uptake in WAT and increased thermogenesis.

Fulvestrant treatment improves the metabolism of diet-induced obese/diabetic mice

Our results using Fulvestrant propose that this pharmacological approach is potentially therapeutic. Whereas ERαKO and OVX females are obese and diabetic, the mice we used so far to test Fulvestrant were raised on normal chow (Figures 3–5). Hence, we utilized a diet-induced diabetes mouse model fed with a high-fat high-sucrose diet (HFD). Aligning with the surgical OVX model, we fed 2-month-old females with HFD for 3 months, and during the last month, we administered Fulvestrant or a vehicle (Figure 6A). As expected, HFD resulted in weight gain (Figure S8A), and Fulvestrant administration had no effect on body weight, fat content, fat mass or lean mass when compared to vehicle treatment (Figures 6B–C and S8A–C). Then, we placed the HFD-fed mice in a cold-chamber for a week or kept them at RT. Following cold-exposure, Fulvestrant-treated females reduced body weight and fat mass compared to vehicle-treated females at RT (Figure 6B and C). The reduction in adiposity in females on HFD was moderate (Figures 6C and S8B, D–E), unlike Fulvestrant treatment in females on normal chow (Figure 4B–G). In accordance with observations in cold-exposed OVX females (Figure S3D), Fulvestrant treatment in females on HFD reduced liver weight following cold-exposure (Figure S8F), but did not affect the weight of other organs (not shown). Although Fulvestrant showed a moderate effect on adiposity, we observed a glucose-lowering effect of Fulvestrant in females on HFD, already evident at RT (Figure 6D). In line with previous reports,[15,16] cold-exposure per se reduced the circulating levels of glucose, cholesterol, triglycerides and insulin in mice on HFD (Figures 6D and S8G–H), however, Fulvestrant treatment had no additive effect. We additionally performed glucose and insulin tolerance tests at RT or following a week of cold-exposure. Cold-exposure is known to increase glucose and insulin tolerance in mice on HFD,[15] which was supported by evaluating vehicle-treated females (Figure 6E and F). Notwithstanding, Fulvestrant treatment in females on HFD had a significant synergistic effect in alleviating glucose intolerance in the cold (Figure 6E) and insulin tolerance at RT (Figure 6F), despite similar insulin levels (Figure S8H). Next, we applied histology and gene expression analyses to females on HFD to evaluate browning/beiging. Histological examination and UCP1 immunoreactivity of SWAT at cold pointed to a scattered emergence of $UCP1^{+}$ multilocular adipocytes, but they were not more abundant in Fulvestrant-treated mice (Figure S8I, Table S2 and not shown). The VWAT of females on HFD was resistant to cold-induced beiging, regardless of treatment (not shown). Already evident at RT, the "whiter" BAT, which characterized vehicle-treated females on HFD, was restored to a normal morphology in Fulvestrant-treated females on HFD (Figure 6G). At cold, BAT morphology appeared even denser in Fulvestrant-treated females on HFD (Figure 6G). On one hand, at cold, Fulvestrant-treated females presented only a moderate elevation in mRNA levels of brown/beige cell markers in SWAT as compared to vehicle-treated females (Figure 6H). On the other hand, the elevation in the expression of these markers was more notable in BAT at cold (Figure 6I). At RT, Fulvestrant-treated females exhibited increased basal mRNA levels of UCP1 in BAT, but not in SWAT (Figure S8J, applies to other genes too – not shown). The histological and gene expression analyses suggest that HFD partially inhibited the enhancing effect of Fulvestrant on cold-induced WAT beiging, but not on BAT. Similarly to Fulvestrant-treated females on normal chow (Figures 5H and S7B), Fulvestrant-treated females on HFD retained a higher body temperature at cold (Figures 6J and S8K). Moreover, in a similar manner to the observations in OVX females (Figures 2J and S4G), we observed correction of HFD-associated hepatosteatosis in Fulvestrant-treated females following cold-exposure (Figures 6K and S8L). In summary, our study demonstrates that estrogen receptor inhibition leads to reduced adiposity and improved glucose metabolism following cold-exposure, which are secondary to enhanced cold-induced beiging/browning.

Estrogen receptor inhibition promotes beiging via β3-adrenoreceptor

Based on our observations, estrogen receptor inhibition enhanced cold-induced beiging. Adipocyte beiging is associated with multiple signaling pathways, predominantly cAMP-mediated pathways.[34] Indeed, Fulvestrant treatment in vitro elevated basal cAMP levels in differentiated beige cells and Forskolin-induced cAMP levels in

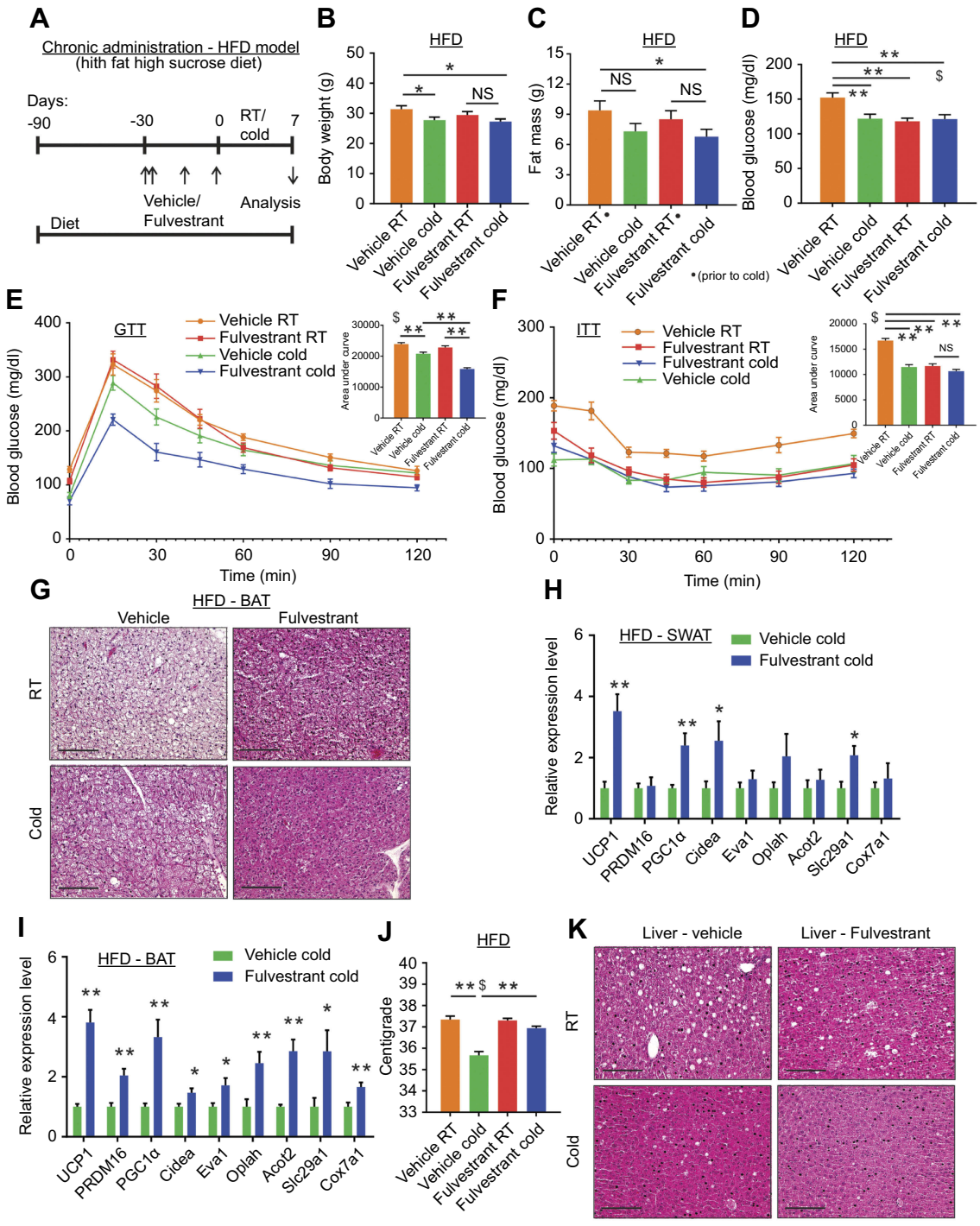

Figure 6 Fulvestrant treatment improves the metabolism of diet-induced obese/diabetic mice. (**A**–**K**) Chronic administration in a high-fat diet (HFD) model: at the age of two-month-old onwards, WT female mice were fed with high-fat high-sucrose diet. Two months later, as described in (**A**), the females were given a vehicle or 40 mg/kg/injection Fulvestrant for a month, then they were subjected to cold-exposure (6 °C) for 7 days or maintained at RT (23 °C). (**B**) Body weight, n≥11. (**C**) Fat mass by NMR, n≥17. (**D**) Blood glucose levels of vehicle-treated and Fulvestrant-treated females on HFD, n≥7. (**E**–**F**) Glucose tolerance (**E**) and insulin tolerance (**F**) tests were performed in vehicle-treated and Fulvestrant-treated females on HFD at RT (a week prior to cold-exposure) and immediately after cold-exposure. Mice were fasted, i.p. injected with 1.25 g/kg glucose (**E**) or 0.75 mU/g insulin (**F**), and their glucose levels were monitored, n≥8. Insets – areas under curve. (**G**) Representative H&E-stained histological sections of BAT, n≥7. (**H**–**I**) Relative mRNA levels, quantified by qPCR, of brown/beige adipocyte markers expressed in SWAT (IGW) (**H**), and BAT (**I**) at cold, n≥6. (**J**) Body temperature (rectal probe) of vehicle-treated and Fulvestrant-treated females on HFD at RT and cold, n≥7. (**K**) Representative H&E-stained histological sections of the liver. Scale bars =100 μm. Error bars indicate S.E.M. Statistical significance assessed by two-tailed Student's *t*-test, **p*<0.05, ***p*<0.01, NS, not significant; and one-way ANOVA test, $^{\$}p$<0.01.

undifferentiated cells (Figures 7A and S9A), suggesting ERα inhibition "primes" cells towards beiging. One of the key stimulants of cAMP-mediated signaling in adipocytes is the sympathetic nervous system, primarily via β-adrenoreceptors.[9,13,34] We therefore examined whether β-adrenoreceptors are upregulated in response to in vitro Fulvestrant treatment. We detected a subtype-restricted upregulation of β3-adrenoreceptor (AdRβ3) in beige cells, regardless of whether Fulvestrant is added during or after differentiation (Figure 7B–D). Fulvestrant treatment of non-induced undifferentiated cells also resulted in an upregulation of β-adrenoreceptors, but not in a subtype-restricted manner (Figure S9B–D). We should emphasize that the mRNA levels of UCP1 and AdRβ3 in undifferentiated cells were inferior to that of differentiated beige cells (Figure S9D), and that UCP1 was absent at the protein level in Fulvestrant-treated undifferentiated cells (not shown). PPARγ2 is an essential transcription factor that drives white/beige adipocyte differentiation.[35–38] In differentiated beige cells, Fulvestrant did not affect PPARγ2 expression (Figure 7B and C), however, Fulvestrant increased its expression in undifferentiated cells (Figure S9B). Considering no effect on cell proliferation (Figure S9E) or adipocyte formation (Figure S5A and B, not shown), these results suggest that Fulvestrant gives a "head-start" in the beiging process. Notably, Fulvestrant is insufficient to trigger beiging by itself, and requires external signals provided by the beige adipogenic media. Could Fulvestrant enhance beiging via AdRβ3 in a similar manner to cold-induced beiging? Since Fulvestrant pre-treatment upregulated AdRβ3 expression (Figures 7D and S9C), we first pre-treated cells with Fulvestrant or a vehicle, and then stimulated the cells with the specific AdRβ3 agonist CL-316,243 in the absence of Fulvestrant. Indeed, Fulvestrant pre-treatment increased the number of $UCP1^{+}$ beige cells in response to stimulation by CL-316,243, whether it is added during differentiation (Figure 7E) or as pre-treatment prior to differentiation (Figure S9F). In other words, Fulvestrant pre-treatment enhanced CL-316,243-induced beiging in vitro. To further support an AdRβ3-mediated effect, we stimulated cultured beige cells by the natural ligand, Norepinephrine (NE). Not only that Fulvestrant enhanced NE-induced beiging, co-treating beige cells with the specific AdRβ3 antagonist SR59230A inhibited NE-induced beiging (Figure 7F). Co-treating the cells with a pan-AdRβ blocker propranolol completely abolished NE-induced beiging (not shown). Next, we tested whether AdRβ3 stimulation in Fulvestrant-treated females and ERαKO females results in enhanced beiging in a similar manner to cold-exposure. Fulvestrant-treated WT females and ERαKO females showed an upregulated AdRβ3 expression in SWAT compared to their control counterparts (Figure S9G–I). We pre-treated 4-month-old female mice with vehicle or Fulvestrant, followed by administration of CL-316,243 injections (Figure 7G). We then evaluated SWAT beiging by histological morphology, UCP1 immunostaining and gene expression analysis. Strikingly, Fulvestrant-pre-treated females demonstrated an enhanced beiging response to CL-316,243 administration as compared to vehicle-pre-treated females (Figure 7H–I, Table S2 and Figure S9J). Despite significant elevation in the expression of brown/beige cell markers in SWAT (Figure S9J), Fulvestrant pre-treatment did not result in a profound effect on BAT (Figure S9K). Finally, ERαKO females demonstrated an enhanced beiging effect in response to CL-316,243 administration (Figure 7J–K, Table S2 and not shown). In summary, estrogen receptor inhibition enhances adipocyte beiging in vitro and in vivo via AdRβ3 upregulation and activation.

Discussion

Mouse models of estrogen or ERα deficiencies often develop diabetes and obesity, characterized by high fat mass, glucose intolerance, insulin resistance, hyperlipidemia and hepatosteatosis.[2–4,24,26,27] In this study, we show that cold-exposure led to reduced adiposity and improved metabolic profile in ERαKO females, OVX females and Fulvestrant-treated females on HFD (summarized in Figure S10A and B). Supported by our results, cold-exposure by itself is capable of improving glucose metabolism in obese/diabetic rodent models.[15] Yet, our results imply that under circumstances of estrogen receptor inhibition, mice experience a further improvement of glucose metabolism in response to cold-exposure. While at "normal" conditions of RT, ERαKO and OVX female mice were obese/diabetic, at cold, they were more susceptible to its metabolic-beneficial effects. In all these models, including regimens of Fulvestrant treatment in female mice, we detected an enhanced cold-induced beiging, predominantly in SWAT, according to histological morphology and gene-expression profiles. We noticed some differences in the manifestation of browning/beiging between these models. For example, cold-induced VWAT beiging occurred only following chronic Fulvestrant pre-treatment in mice on normal-chow. On the other hand, Fulvestrant pre-treatment in mice on HFD resulted in a mild cold-induced SWAT beiging, attaining stronger effects on BAT. While it is conceivable that the enhanced cold-induced beiging and BAT activity exert the observed

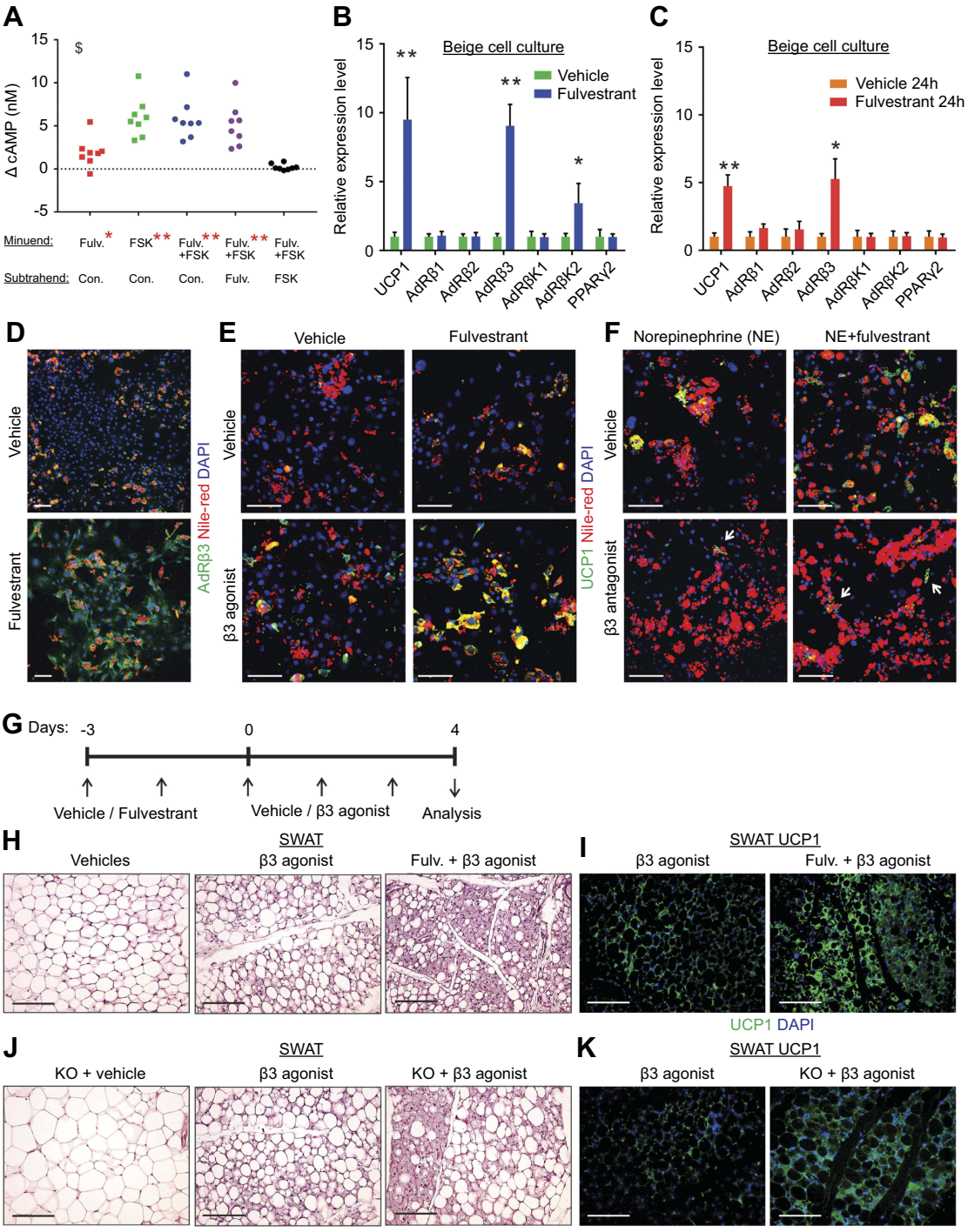

Figure 7 Estrogen receptor inhibition promotes beiging via β3-adrenoreceptor. (**A**–**F**) SV cells were isolated from SWAT of two-month-old WT females. Confluent cells were induced with beige adipogenic media. A week later, the following experiments were performed. (**A**) Relative changes in cAMP concentrations upon induction with or without Forskolin. Every dot represents an average of technical triplicates of one biological sample. The relative changes in cAMP concentrations are calculated as differences between treatments, n≥8. (**B**–**C**) Relative mRNA levels, quantified by qPCR, of UCP1, β-adrenergic receptors, β-adrenergic receptor kinases and PPARγ2. (**B**) Vehicle or Fulvestrant were added during differentiation, then the differentiated beige cells were activated with Forskolin for 8 hr, n≥7. (**C**) Vehicle or Fulvestrant were added to differentiated beige cells for 24 hr without Forskolin, n≥5. (**D**–**F**) Vehicle or Fulvestrant were added during differentiation. Nile Red stains lipid droplets. (**D**) Vehicle-treated or Fulvestrant-treated beige cells were immunostained for AdRβ3 expression. (**E**) Vehicle-treated or Fulvestrant-treated beige cells were activated or not with CL-316,243 (β3 agonist) for 24 hr, and then immunostained for UCP1 expression. (**F**) Vehicle-treated or Fulvestrant-treated beige cells were activated with Norepinephrine (NE) for 24 hr; concomitantly co-treated with a vehicle or SR59230A (β3 antagonist), and then immunostained for UCP1 expression. (**G**–**I**) Four-month-old WT females were pre-treated with a vehicle or 40 mg/kg/injection Fulvestrant, followed by administration of 1 mg/kg/day β3 agonist as described in (**G**). Representative histological sections of SWAT, which were either H&E-stained (**H**), n≥8, or immunostained for UCP1 expression (**I**). (**J**–**K**) Four-month-old ERαWT or ERαKO (KO) females were treated with β3 agonist as described in (**G**). Representative histological sections of SWAT, which were either H&E-stained (**J**), n≥7, or immunostained for UCP1 expression (**K**). Scale bars =100 μm. Error bars indicate S.E.M. Statistical significance assessed by two-tailed Student's *t*-test, **p*<0.05, ***p*<0.01; and one-way ANOVA test, $^{\$}p$<0.01. In (**A**), results are based on a matched standard curve and a linear regression analysis.

beneficial effects on glucose metabolism, we cannot exclude that other tissues with altered estrogen signaling play a cold-inducible role. It is also possible that ERβ or indirect non-estrogenic signaling events shape the physiological outcome. Tissue-specific ERα mutants, such as deletions of ERα in mature adipocytes, hepatocytes, skeletal muscle and hypothalamic neurons, have been shown to partially develop characteristics of metabolic dysfunction.[18,39–41] Estrogen-dependent regulation of energy balance by the central nervous system is a key physiological contributor, and may explain in part the obese/diabetic phenotype of whole-body ERαKO and OVX mice.[41–43] Thus, it is not surprising that Estradiol administration in OVX female mice protects them from obesity and glucose intolerance.[5] Taking into account the pleiotropic roles of Estrogen in energy balance, we did not test its effects in OVX mice at cold, which may result in synergism rather than reversal of effects. Nonetheless, Fulvestrant, which does not appear to cross the blood-brain-barrier,[28] has an advantage over other SERMs in our understating of central vs peripheral roles of ERα. In support, cerebroventricular injections of Fulvestrant reduce body weight,[44] whereas peripheral injections do not.[28] What's more, Fulvestrant downregulates ERα expression,[29,30] including in our study, and therefore serves as a reliable model for ERα deficiency. We presented a cell-autonomous beiging response under conditions of ERα deficiency by utilizing an isolated primary cell culture. We previously reported an enhanced beiging in mice with an adipose-lineage-specific deletion of ERα,[8] and herein we further validate this beiging effect in mice with systemic ERα-deficiency followed by stimuli of beiging/browning. These stimuli, elicited by cold-exposure or adrenergic signals, are necessary to amplify the downstream signaling triggered by ERα inhibition, which do not generate a beiging phenotype under non-stimulatory conditions (ie RT). This unknown downstream signaling is yet to be elucidated, however, our preliminary findings indicated upregulated cAMP levels, which are a driving force in beiging, as well as an increased AdRβ3 expression. Although AdRβ3 signaling triggers prominent beiging,[13,34,45] AdRβ3-KO mice and mice treated with AdRβ3 antagonist display normal cold-induced beiging,[46,47] suggesting AdRβ3 is redundant in the specific response to cold-exposure. The findings in this study are not contradictory, since they propose that following ERα inhibition, brown/beige adipocytes are more sensitive to activation rather than depend on AdRβ3. This increased sensitivity may occur both at the immature and mature cell level (Figure S10C), although this cellular mechanism should be further validated in vivo. Altogether, our results suggest that pre-clinical mouse models of post-menopause have a propensity to increased beiging and improved metabolism upon cold-exposure. Thus, we conclude that cold-exposure has a clinical potential in obese/diabetic postmenopausal patients.

Acknowledgments

We thank Dr Jonathan M Graff for supporting this work and giving fruitful advice. Additionally, we thank Brianna Findley and Xiaoli Lin from the Radiology & Advanced Imaging Research Center for their assistance in conducting the glucose uptake assay. This study was supported by National Institutes of Health, National Institute of Diabetes and Digestive and Kidney Diseases (NIH, NIDDK R01 DK066556 and R01 DK088220) and the American Heart Association postdoctoral fellowship grant (KL, 16POST27250024).

Disclosure

The authors report no conflicts of interest in this work.

References

1. Lovre D, Lindsey SH, Mauvais-Jarvis F. Effect of menopausal hormone therapy on components of the metabolic syndrome. *Ther Adv Cardiovasc Dis*. 2017;11:33–43.
2. Palmer BF, Clegg DJ. The sexual dimorphism of obesity. *Mol Cell Endocrinol*. 2015;402:113–119. doi:10.1016/j.mce.2014.11.029
3. Heine PA, Taylor JA, Iwamoto GA, Lubahn DB, Cooke PS. Increased adipose tissue in male and female estrogen receptor-alpha knockout mice. *Proc Natl Acad Sci U S A*. 2000;97(23):12729–12734. doi:10.1073/pnas.97.23.12729
4. Pallier E, Aubert R, Lemonnier D. Effect of diet and ovariectomy on adipose tissue cellularity in mice. *Reprod Nutr Dev*. 1980;20(3A):631–636.
5. Stubbins RE, Holcomb VB, Hong J, Nunez NP. Estrogen modulates abdominal adiposity and protects female mice from obesity and impaired glucose tolerance. *Eur J Nutr*. 2012;51(7):861–870. doi:10.1007/s00394-011-0266-4
6. Stefanick ML. Postmenopausal hormone therapy and cardiovascular disease in women. *Nutr Metab Cardiovasc Dis*. 2010;20(6):451–458. doi:10.1016/j.numecd.2010.02.015
7. Rozenberg S, Vandromme J, Antoine C. Postmenopausal hormone therapy: risks and benefits. *Nat Rev Endocrinol*. 2013;9(4):216–227. doi:10.1038/nrendo.2013.17
8. Lapid K, Lim A, Clegg DJ, Zeve D, Graff JM. Oestrogen signalling in white adipose progenitor cells inhibits differentiation into brown adipose and smooth muscle cells. *Nat Commun*. 2014;5:5196. doi:10.1038/ncomms5972
9. Townsend KL, Tseng YH. Of mice and men: novel insights regarding constitutive and recruitable brown adipocytes. *Int J Obes Suppl*. 2015;5(Suppl 1):S15–S20. doi:10.1038/ijosup.2015.5
10. Thyagarajan B, Foster MT. Beiging of white adipose tissue as a therapeutic strategy for weight loss in humans. *Horm Mol Biol Clin Investig*. 2017;31:2.
11. Kim SH, Plutzky J. Brown fat and browning for the treatment of obesity and related metabolic disorders. *Diabetes Metab J*. 2016;40(1):12–21. doi:10.4093/dmj.2016.40.1.12

12. Stanford KI, Middelbeek RJ, Townsend KL, et al. Brown adipose tissue regulates glucose homeostasis and insulin sensitivity. *J Clin Invest*. 2013;123(1):215–223. doi:10.1172/JCI62308
13. Wang W, Seale P. Control of brown and beige fat development. *Nat Rev Mol Cell Biol*. 2016;17(11):691–702. doi:10.1038/nrm.2016.96
14. Hanssen MJ, Hoeks J, Brans B, et al. Short-term cold acclimation improves insulin sensitivity in patients with type 2 diabetes mellitus. *Nat Med*. 2015;21(8):863–865. doi:10.1038/nm.3891
15. Vallerand AL, Lupien J, Bukowiecki LJ. Cold exposure reverses the diabetogenic effects of high-fat feeding. *Diabetes*. 1986;35(3):329–334. doi:10.2337/diab.35.3.329
16. Bartelt A, Bruns OT, Reimer R, et al. Brown adipose tissue activity controls triglyceride clearance. *Nat Med*. 2011;17(2):200–205. doi:10.1038/nm.2297
17. Johnston SJ, Cheung KL. Fulvestrant - a novel endocrine therapy for breast cancer. *Curr Med Chem*. 2010;17(10):902–914.
18. Davis KE, M DN, Sun K, et al. The sexually dimorphic role of adipose and adipocyte estrogen receptors in modulating adipose tissue expansion, inflammation, and fibrosis. *Mol Metab*. 2013;2(3):227–242. doi:10.1016/j.molmet.2013.05.006
19. Berglund ED, Li CY, Poffenberger G, et al. Glucose metabolism in vivo in four commonly used inbred mouse strains. *Diabetes*. 2008;57(7):1790–1799. doi:10.2337/db07-1615
20. Berry DC, Jiang Y, Arpke RW, et al. Cellular aging contributes to failure of cold-induced beige adipocyte formation in old mice and humans. *Cell Metab*. 2017;25(1):166–181. doi:10.1016/j.cmet.2016.10.023
21. Tang W, Zeve D, Suh JM, et al. White fat progenitor cells reside in the adipose vasculature. *Science*. 2008;322(5901):583–586. doi:10.1126/science.1156232
22. Bäcker V ImageJ macro tool sets for biological image analysis. ImageJ User and Developer Conference 2012; 24–26 October 2012, Luxembourg.
23. Parlee SD, Lentz SI, Mori H, MacDougald OA. Quantifying size and number of adipocytes in adipose tissue. *Methods Enzymol*. 2014;537:93–122. doi:10.1016/B978-0-12-411619-1.00006-9
24. Ribas V, Nguyen MT, Henstridge DC, et al. Impaired oxidative metabolism and inflammation are associated with insulin resistance in ERalpha-deficient mice. *Am J Physiol Endocrinol Metab*. 2010;298(2):E304–E319. doi:10.1152/ajpendo.00504.2009
25. Rabii J, Ganong WF. Responses of plasma "estradiol" and plasma LH to ovariectomy, ovariectomy plus adrenalectomy, and estrogen injection at various ages. *Neuroendocrinology*. 1976;20(3):270–281. doi:10.1159/000122491
26. Vieira Potter VJ, Strissel KJ, Xie C, et al. Adipose tissue inflammation and reduced insulin sensitivity in ovariectomized mice occurs in the absence of increased adiposity. *Endocrinology*. 2012;153(9):4266–4277. doi:10.1210/en.2011-2006
27. Zhu L, Brown WC, Cai Q, et al. Estrogen treatment after ovariectomy protects against fatty liver and may improve pathway-selective insulin resistance. *Diabetes*. 2013;62(2):424–434. doi:10.2337/db11-1718
28. Wade GN, Blaustein JD, Gray JM, Meredith JM. ICI 182, 780:a pure antiestrogen that affects behaviors and energy balance in rats without acting in the brain. *Am J Physiol*. 1993;265(6 Pt 2):R1392–R1398. doi:10.1152/ajpregu.1993.265.6.R1392
29. Pink JJ, Jordan VC. Models of estrogen receptor regulation by estrogens and antiestrogens in breast cancer cell lines. *Cancer Res*. 1996;56(10):2321–2330.
30. Howell A, Osborne CK, Morris C, Wakeling AE. ICI 182,780 (Faslodex): development of a novel, "pure" antiestrogen. *Cancer*. 2000;89(4):817–825. doi:10.1002/1097-0142(20000815)89:4<817::aid-cncr14>3.0.co;2-6
31. Jeong S, Yoon M. 17beta-Estradiol inhibition of PPARgamma-induced adipogenesis and adipocyte-specific gene expression. *Acta Pharmacol Sin*. 2011;32(2):230–238. doi:10.1038/aps.2010.198
32. Eaton GJ, Johnson FN, Custer RP, Crane AR. The Icr: Ha(ICR) mouse: a current account of breeding, mutations, diseases and mortality. *Lab Anim*. 1980;14(1):17–24. doi:10.1258/002367780780943141
33. Robertson JF, Odling-Smee W, Holcombe C, Kohlhardt SR, Harrison MP. Pharmacokinetics of a single dose of fulvestrant prolonged-release intramuscular injection in postmenopausal women awaiting surgery for primary breast cancer. *Clin Ther*. 2003;25(5):1440–1452.
34. Shi F, Collins S. Second messenger signaling mechanisms of the brown adipocyte thermogenic program: an integrative perspective. *Horm Mol Biol Clin Investig*. 2017;31:2.
35. Tontonoz P, Hu E, Spiegelman BM. Stimulation of adipogenesis in fibroblasts by PPAR gamma 2, a lipid-activated transcription factor. *Cell*. 1994;79(7):1147–1156. doi:10.1016/0092-8674(94)90006-x
36. Chawla A, Schwarz EJ, Dimaculangan DD, Lazar MA. Peroxisome proliferator-activated receptor (PPAR) gamma: adipose-predominant expression and induction early in adipocyte differentiation. *Endocrinology*. 1994;135(2):798–800. doi:10.1210/endo.135.2.8033830
37. Berry DC, Jiang Y, Graff JM. Mouse strains to study cold-inducible beige progenitors and beige adipocyte formation and function. *Nat Commun*. 2016;7:10184. doi:10.1038/ncomms10184
38. Ohno H, Shinoda K, Spiegelman BM, Kajimura S. PPARgamma agonists induce a white-to-brown fat conversion through stabilization of PRDM16 protein. *Cell Metab*. 2012;15(3):395–404. doi:10.1016/j.cmet.2012.01.019
39. Qiu S, Vazquez JT, Boulger E, et al. Hepatic estrogen receptor alpha is critical for regulation of gluconeogenesis and lipid metabolism in males. *Sci Rep*. 2017;7(1):1661. doi:10.1038/s41598-017-01937-4
40. Ribas V, Drew BG, Zhou Z, et al. Skeletal muscle action of estrogen receptor alpha is critical for the maintenance of mitochondrial function and metabolic homeostasis in females. *Sci Transl Med*. 2016;8(334):334ra354. doi:10.1126/scitranslmed.aaf0746
41. Xu Y, Nedungadi TP, Zhu L, et al. Distinct hypothalamic neurons mediate estrogenic effects on energy homeostasis and reproduction. *Cell Metab*. 2011;14(4):453–465. doi:10.1016/j.cmet.2011.08.009
42. Xu P, Cao X, He Y, et al. Estrogen receptor-alpha in medial amygdala neurons regulates body weight. *J Clin Invest*. 2015;125(7):2861–2876. doi:10.1172/JCI80941
43. Xu Y, O'Malley BW, Elmquist JK. Brain nuclear receptors and body weight regulation. *J Clin Invest*. 2017;127(4):1172–1180. doi:10.1172/JCI88891
44. Martinez de Morentin PB, Gonzalez-Garcia I, Martins L, et al. Estradiol regulates brown adipose tissue thermogenesis via hypothalamic AMPK. *Cell Metab*. 2014;20(1):41–53. doi:10.1016/j.cmet.2014.03.031
45. Cousin B, Cinti S, Morroni M, et al. Occurrence of brown adipocytes in rat white adipose tissue: molecular and morphological characterization. *J Cell Sci*. 1992;103(Pt 4):931–942.
46. de Jong JMA, Wouters RTF, Boulet N, Cannon B, Nedergaard J, Petrovic N. The beta3-adrenergic receptor is dispensable for browning of adipose tissues. *Am J Physiol Endocrinol Metab*. 2017;312(6):E508–E518. doi:10.1152/ajpendo.00437.2016
47. Jiang Y, Berry DC, Graff JM. Distinct cellular and molecular mechanisms for beta3 adrenergic receptor-induced beige adipocyte formation. *Elife*. 2017;6. doi:10.7554/eLife.30329